# Calorimetric Investigation of the Structural Relaxation of Amorphous Materials: Evaluating Validity of the Methodologies

**KOHSAKU KAWAKAMI, MICHAEL J. PIKAL**

Department of Pharmaceutical Sciences, School of Pharmacy, University of Connecticut, 372 Fairfield Road, Storrs, Connecticut 06269

*Received 4 June 2004; revised 27 July 2004; accepted 18 November 2004*

*Published online in Wiley InterScience (www.interscience.wiley.com). DOI 10.1002/jps.20298*

**ABSTRACT:** Although the potential advantages of the amorphous solid state is widely recognized among pharmaceutical researchers, its industrial applications have been mainly limited to freeze-dried injectable formulations where the amorphous form is naturally produced. Applications in oral dosage forms have been limited due, at least in part, to the poor state of knowledge regarding physical properties and stability of amorphous materials. Relaxation behavior is perhaps one of the most important physical characteristics of amorphous materials because relaxation kinetics are closely related to physical and chemical stability. Although recent developments in calorimetry methodology have facilitated detailed characterization of relaxation behavior, some experimental difficulties remain, and quantitative analysis of structural relaxation is still under development. This review focuses on the calorimetric investigation of the structural relaxation of drugs and excipients, and discusses the difficulties in the experimental evaluation of the relaxation time by those methods. We also present an original investigation of the impact of increases in relaxation time during an annealing experiment on the values of relaxation time, $\tau$, and stretched exponential constant, $\beta$, obtained from analysis of the experiment according to the Kohlraush-Williams-Watts kinetic model. Using results from a numerical simulation, we find that the values of $\tau$ and $\beta$ obtained from the data analysis are too large and too small, respectively, but the value of stretched relaxation time, $\tau^{\beta}$, remains reliable. The time dependence of the relaxation time is likely to play an important role in the non-Arrhenius behavior of pharmaceutical glasses.

**Keywords:** amorphous; glass; enthalpy relaxation; relaxation time; enthalpy recovery; temperature-modulated DSC; isothermal microcalorimetry; glass transition; Kohlrausch-Williams-Watts (KWW) equation; modified stretched exponential (MSE) equation

## INTRODUCTION

Improvements in formulation technology are becoming more critical in the development of poorly soluble compounds, where oral bioavailability is typically low. Low bioavailability may become an economic issue because of higher manufacturing costs arising from the need to use more drug substance when much of the drug is not bioavailable. Moreover, low-bioavailable drugs may cause serious side effects, if an abnormally large amount is absorbed due to patient specific effects or other factors. In such cases, it may be advantageous to abandon the crystalline state and employ special high solubility dosage forms, such as amorphous solid dispersions or microemulsions, despite the fact that the crystalline

Kohsaku Kawakami's present address is Pharmaceutical Research & Development, Banyu Pharmaceutical Co., Ltd. 810 Nishijo, Menuma-machi, Saitama 360-0214, Japan.

*Correspondence to*: Kohsaku Kawakami (Telephone: 81-48-588-8791; Fax: 81-48-588-4695;
E-mail: kohsaku_kawakami@merck.com)

Journal of Pharmaceutical Sciences, Vol. 94, 948–965 (2005)

state is usually the most stable form physically and chemically.[1–3] However, the state of knowledge regarding these special dosage forms is still poor, and partly because of this lack of knowledge, development organizations are hesitant to employ this technology. Thus, the applications of amorphous solid technology has been limited mainly to freeze-dried parenteral formulations.

Despite a significant amount of research focused on amorphous materials, the physical properties of amorphous solids, such as the glass transition and structural relaxation dynamics, are not fully understood. As an amorphous solid, or glass, is held below its glass transition temperature, the material relaxes toward the quasi equilibrium, or "metastable," supercooled liquid state, thereby decreasing in energy, entropy, and free volume during this relaxation process. This process is called structural relaxation,[4–6] and is a result of the fact that a glassy material is in a nonequilibrium state with significant molecular mobility on the time scale of the relaxation experiment. It should be noted that structural relaxation may arise from various types of perturbations such as electric field, magnetic field, mechanical force, and laser light, but only relaxation resulting from thermal perturbations will be discussed in this review. Because the dynamics of structural relaxation is an indicator of molecular mobility, and because degradation processes invariably involve molecular mobility of some type, physical/chemical stability and relaxation dynamics may well be closely related. Many techniques, such as differential scanning calorimetry (DSC),[7–9] dielectric relaxation,[7,10] and mechanical analysis,[11,12] have been applied in studies of relaxation phenomena. Modulated temperature DSC (MTDSC) is perhaps the most common technique used for investigating the relaxation of pharmaceutical amorphous solids.[13–19] With DSC techniques, an aged sample is heated through the glass transition, and the enthalpy lost during relaxation is measured as an enthalpy recovery event superimposed on the heat capacity change at the glass transition. MTDSC is a special DSC technique where a sinusoidal variation in temperature is superimposed on the linear temperature ramp. This feature allows separation of the glass transition event from the enthalpy recovery endotherm, thereby facilitating measurement of enthalpy recovery. Isothermal microcalorimetry, which has been employed to investigate various characteristics of pharmaceutical solids,[20–23] is also a powerful calorimetry technique for investigation of the relaxation process. Isothermal calorimetry allows one to directly observe the rate of energy loss during enthalpy relaxation and has the advantage of superior sensitivity relative to the DSC techniques.[24,25] This review focuses on calorimetric investigations of the structural relaxation and discusses the resolution of experimental difficulties associated with the quantitative characterization of structural relaxation dynamics.

## GENERAL THEORY OF RELAXATION

### Basic Relaxation Theory (KWW Equation)

Figure 1 shows a schematic of an enthalpy-temperature diagram of an amorphous system. When a liquid is cooled, it usually crystallizes below the melting temperature $T_m$. However, when the cooling rate is sufficiently fast, the liquid fails to crystallize and the supercooled state is attained. Although the supercooled liquid is a nonequilibrium state relative to the crystalline state, it is an equilibrium state with respect to structural changes with temperature. That is, cooling causes essentially instantaneous corresponding changes in structure and thermodynamic properties, so the supercooled liquid is said to be in "structural equilibrium." Further cooling to below the glass transition temperature $T_g$ causes the system to fall out of structural equilibrium as the time scale for structural rearrangements within the material become too slow to keep up with cooling. At this point, the state is called a glass. Below the glass transition temperature, the state defined by the continuation of the supercooled liquid line is essentially a "virtual state" because it represents the glassy state that is also in structural equilibrium. This state, we refer to as the "equilibrium glassy state." A real glass may approach this equilibrium state asymptotically during an annealing process. This approach to the equilibrium glassy state characterized by the extension of the supercooled liquid line is shown by an arrow (a). This spontaneous process is called relaxation. Relaxation may consist of more than two different modes. Structural relaxation (α-relaxation) and Johari-Goldstein relaxation (β-relaxation)[5,26,27] are the representative relaxation modes that have been studied extensively. Structural relaxation or "α-relaxation" reflects motion of the whole molecule such as diffusional motion and viscous flow while "β-relaxation" or Johari-Goldstein relaxation is usually believed to originate from intramolec-

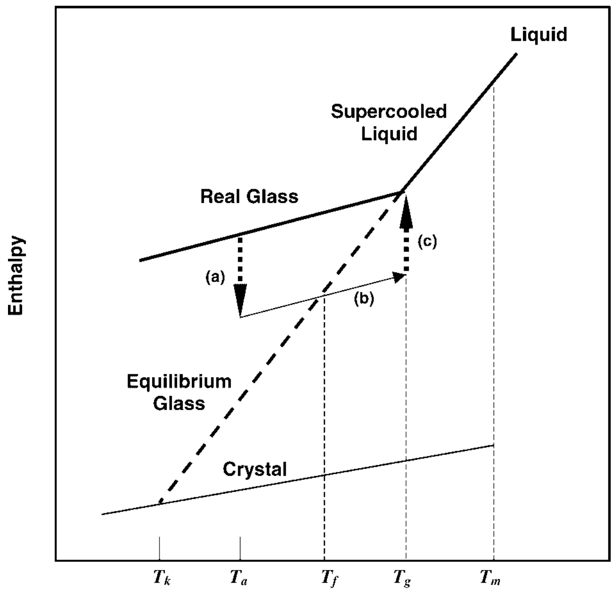


**Figure 1.** Enthalpy-temperature diagram of solids. $T_m$ is the equilibrium melting point, $T_g$ is the glass transition temperature, $T_f$ is the fictive temperature, $T_a$ is the annealing temperature, and $T_k$ is the Kauzmann (or zero mobility) temperature.

ular motion, such as rotation of a side chain on a polymer or motion of a small group of atoms on a large molecule that is not coupled or correlated with motion of the entire molecule. In this review, we discuss only structural relaxation ($\alpha$-relaxation), which to date has been the process of greatest interest among pharmaceutical researchers and is easiest to study using calorimetric techniques.

Thermodynamic properties, such as enthalpy or volume, change during annealing as if the system were an ensemble of independent subsystems, each undergoing exponential relaxation with a unique time constant. The overall decay function $\phi$ can be written as

$$\phi(t,T) = \sum_i g_i \exp\left(-\frac{t}{\tau_i(T)}\right) \quad (1)$$

where $g_i$, $T$, and $t$ are the weighting factor, temperature, and time, respectively. The weighting factor is essentially the probability that a given subsystem has relaxation time, $\tau_i$, and therefore, $g_i$ defines the "distribution of states." The relaxation time is normally around 100 s at the glass transition temperature,[28] and becomes significantly larger at lower temperatures. Empirically, a summation of exponential decay functions may be *approximated* by the "stretched exponential" function,

$$\phi_{\mathrm{KWW}}(t,T) = \exp\left[-\left(\frac{t}{\tau(T)}\right)^{\beta}\right] \quad (2)$$

This equation is commonly used because of its simplicity and is called the Kohlrausch-Williams-Watts (KWW) equation.[4–6] The KWW equation is an empirical equation, although some attempts have been made to provide a theoretical rationalization for the form.[29] The parameter, $\beta$, which may take on values between 0 and 1, is usually taken as a reflection of the distribution of substates.[30] That is, when $\beta$ is near unity, the distribution of states is narrow, while a value of $\beta$ much less than unity would mean a broad distribution of states (i.e., a significant population of substates with widely divergent relaxation times). However, it should be noted that other interpretations are possible. The existence of a highly cooperative process is also said to contribute to a value of $\beta$ less than unity.[19,31] The value of $\beta$ is also said to reflect the dimensionality of diffusion.[29,32] It should also be noted that there are many empirical ways to analyze the relaxation behavior,[6] although the KWW equation has been the most common approach.

The decay of excess enthalpy during aging can be expressed as

$$H_{\mathrm{ex}}(t,T) = H_{\mathrm{ex}}(0,T)\phi_{\mathrm{KWW}}(t,T) \quad (3)$$

where $H_{\mathrm{ex}}$ is the excess enthalpy, meaning the difference between the enthalpy of the real glass at temperature, $T$, and time, $t$, and the "equilibrium" state of the glass at infinite annealing time (i.e., enthalpy of the equilibrium supercooled liquid). Commonly, the initial excess enthalpy is calculated from

$$H_{\mathrm{ex}}(0,T) = \int_T^{T_g} \Delta C_p dT \quad (4)$$

where $\Delta C_p$ is the heat capacity difference between the real and the equilibrium glass. Ignoring any temperature dependence in $\Delta C_p$ then leads to the approximate expression,

$$H_{\mathrm{ex}}(0,T) = \Delta C_p (T_g - T) \quad (5)$$

Equation 4 also implicitly assumes that the glass is created in a manner equivalent to quench cooling a liquid, thereby ignoring any loss in configurational energy between the glass transition temperature and the final temperature of interest. With these approximations, the measurement of $T_g$ and the heat capacity change at $T_g$ allows calculation of the excess enthalpy at $T$. The enthalpy lost during annealing can be evaluated from a DSC experiment. A sample is allowed to anneal and "relax" for a given time at temperature, $T_a$, and the energy decreases as indicated by the arrow (a) (Fig. 1). Next, the sample is heated along line (b), and when the temperature is near $T_g$ and molecular mobility in the sample is again high, the enthalpy recovers to the supercooled liquid state as shown by arrow (c). This recovery event is observed in the DSC measurement as an endothermic peak. Assuming that the enthalpy relaxation and recovery are the same (i.e., the lengths of arrows (a) and (c) are equal), the relaxation enthalpy value, $H_{ex}(0, T) - H_{ex}(t, T)$, is obtained. This process is repeated for a number of annealing times, and the relaxation time $\tau$ and the stretched exponential parameter $\beta$ can be obtained by fitting eq. 3 to the data using nonlinear regression analysis.

Although the physical meaning of $\beta$ is still ambiguous, it is normally conceded that at least a very low $\beta$ value means a wide distribution of relaxation times $\tau$, for the constituent substates.[34–37] If we assume a log-normal distribution for the relaxation time, the distribution function $g_i$ is written as

$$g_i(x_i) = \frac{1}{\sqrt{2\pi}\sigma}\exp\left(-\frac{x_i^2}{2\sigma^2}\right) \quad (6)$$

where

$$x_i = \ln\left(\frac{\tau_i}{\tau'}\right) \quad (7)$$

Here, $\sigma$, $\tau_i$ and $\tau$ are the standard deviation of $x_i$, the relaxation time for substate $i$ and the most probable relaxation time. In the analysis of relaxation kinetics in terms of the KWW equation, it is not uncommon to obtain $\beta$ values lower than 0.4. However, with the log-normal distribution assumption, a $\beta$ value this low would corresponds to $\sigma > 2$, which is a very broad distribution.[30] In many cases, $\beta$ seems to involve not only the distribution of relaxation times but also reflects other factors that stretch the decay function and reduce the value of $\beta$. One factor that stretches the decay function is the dependence of $\tau$ on the structure of the system.[6,38–40] That is, the relaxation time for each subsystem is *increasing* during the annealing process. This fact is important information for those developing amorphous formulations, because an increase in relaxation time means a decrease in molecular mobility, which often shows a close relationship with chemical/physical stability. A quantitative study on the increase in $\tau$ during relaxation will be provided in a later section.

### Relaxation in the Short-Time Limit (MSE Equation)

The KWW equation is not consistent with physical reality in the short-time limit.[24,41] This problem arises because the first derivative of the KWW equation approaches infinity as time approaches zero. This "infinite initial relaxation rate" is *not* a property of a summation of exponential expressions (i.e., derivative of eq. 1) and is physically unacceptable. To overcome this problem, a modified stretched exponential (MSE) equation was proposed.[24,41]

$$\phi_{MSE}(t, T) = \exp\left[-\left(\frac{t}{\tau_0(T)}\right)\left(1 + \frac{t}{\tau_1(T)}\right)^{\beta-1}\right] \quad (8)$$

As time approaches zero, $\tau_0$ is the relaxation constant that describes relaxation behavior, and $\tau_1$ is another relaxation time constant. $\tau_1$ may also be regarded as a parameter that indicates the length of the "short-time limit," where the KWW equation is not applicable. The constant, $\beta$, has the same meaning as in the KWW expression. The MSE equation was originally derived to characterize relaxation behavior in NMR experiments.[41] At long times, eq. 8 reduces to the same form as the KWW equation, eq. 2, but with the KWW relaxation time $\tau$ replaced by the MSE equivalent, $\tau_D$, where

$$\tau_D = \left(\tau_0\tau_1^{\beta-1}\right)^{1/\beta} \quad (9)$$

Therefore, $\tau_D$ corresponds to (but is not exactly equivalent to) the relaxation time in the KWW equation. At very short times ($t \ll \tau_1$), the MSE equation can be rewritten as

$$\phi(t, T) = \exp\left(-\frac{t}{\tau_0(T)}\right) \quad (10)$$

which shows single-exponential behavior, and thus the first derivative remains finite. In the long-time region ($t \gg \tau_1$), the MSE equation becomes

$$\phi(t, T) = \exp\left[-\left(\frac{t}{\tau_D(T)}\right)^{\beta}\right] \quad (11)$$

This equation is identical with the KWW equation. The MSE equation is useful when the initial relaxation behavior of a material with large relaxation time is analyzed. This matter will be discussed again later.

### The Impact of Changes in Relaxation Time during Annealing on the Determination of $\tau$ and $\beta$

As discussed in the preceding sections, the KWW equation is frequently used to represent the kinetics of structural relaxation, and therefore to serve as the foundation for evaluation of the structural relaxation time from DSC or isothermal calorimetry experiments.[24,42] However, this practice assumes the structural relaxation time is essentially independent of time, which is not correct. During the annealing process required to generate the calorimetric data for kinetic analysis, the sample is decreasing in energy and free volume, and therefore, the structural relaxation time is increasing. The question becomes, "what is the impact of this phenomenon on the values of $\tau$ and $\beta$ evaluated from the KWW equation?" In this section, we address this question by generating enthalpy data as a function of aging time by theoretical calculation or simulation. Next, we "fit" the KWW equation in either the enthalpy or power form to the simulated data to obtain "experimental" values of $\tau$ and $\beta$, as one would do with actual experimental enthalpy or power data, and then compare these values of $\tau$ and $\beta$ to the initial values used in the simulation.

To carry out the simulations, we use the modified Vogel-Tamman-Fulcher equation[4,43] to describe the time dependence of the structural relaxation time, $\tau$, through the time dependence of the fictive temperature, $T_f$,

$$\tau(T, T_f) = \tau_0 \exp\left(\frac{DT_0}{T - (T/T_f)T_0}\right) \tag{12}$$

where $D$ is Angell's strength parameter, and $T_0$ is the "zero mobility temperature." $T_0$ seems to be equivalent to the Kauzmann temperature, $T_k$,[4] and is frequently lower than the glass transition temperature, $T_g$, by about 50 °C. The glass transition, the zero mobility temperature, and the strength parameter are related by,[44]

$$\frac{T_g}{T_0} = 1 + 0.0271 \cdot D \tag{13}$$

The fictive temperature is the temperature at which the equilibrium supercooled liquid has the same configurational entropy (or enthalpy) as the real glass at the temperature of interest (note that here we ignore the small difference between the definition of fictive temperature based upon entropy and the definition based upon enthalpy, because it does not affect results obtained in the simulation). In Figure 1, the fictive temperature is the temperature at the intersection of the iso-configurational enthalpy line, line (b), with the equilibrium supercooled liquid line. Because the fictive temperature decreases toward the actual temperature, $T_a$, during aging, the relaxation time is not constant as the KWW equation assumes. Rather, one must use the integral form of the relaxation function, $\Phi$, to describe the kinetics of enthalpy relaxation.[4,43,45]

$$\Phi(t) = \exp[-I(t)^{\beta}] \tag{14}$$

where $I(t)$ is the integral time average ratio of time to relaxation time,

$$I(t) = \int_0^t \frac{dt'}{\tau(T, T_f)} \tag{15}$$

For a system initially at fictive temperature, $T_f^0$, which is subjected to an instantaneous temperature drop to the annealing temperature $T_a$, we express the relaxation function, $\Phi(t)$, in terms of the time-dependent fictive temperature, $T_f(t)$, by[4,43,45]

$$\Phi(t) = \frac{T_f(t) - T_a}{T_f^0 - T_a} \tag{16}$$

The initial fictive temperature is evaluated by,[46]

$$\frac{1}{T_f^0} = \frac{\gamma}{T_g} + \frac{1-\gamma}{T} \tag{17}$$

$$\gamma = \frac{C_p^l - C_p^g}{C_p^l - C_p^{\text{xstal}}} = \frac{\Delta C_p}{C_p^l - C_p^{\text{xstal}}}$$

where $C_p^l$, $C_p^g$, and $C_p^{\text{xstal}}$ are the heat capacities of liquid, glass, and crystal, respectively.

The simulation proceeds from the following set of initial values: $T_f = T_f^0$, $\Phi = 1$, $\tau$ = calculated from eq. 12 at fictive temperature, $T_f^0$, and $I(t) = 0$. The parameter is then incremented by a differential change corresponding to the differential increment in time, $dt$. Thus, for the $n$th time step, where $n = 1,2,3,\ldots,N$:

$$\begin{aligned} t &= n \cdot dt \\ dI(n) &= dt/\tau(n-1) \\ I(n) &= I(n-1) + dI(n) \\ d\Phi(n) &= -\Phi(n-1) \cdot \beta \cdot I(n)^{(\beta-1)} \\ \Phi(n) &= \Phi(n-1) + d\Phi(n) \\ dT_f(n) &= (T_f^0 - T_a) \cdot d\Phi(n) \\ T_f(n) &= T_f(n-1) + dT_f(n). \end{aligned} \tag{18}$$

Simulations were carried out for annealing at 40 and 50°C for both a "sucrose-like" material and a "trehalose-like" material. Parameters for the sucrose-like material ($T_g = 348$ K, $D = 7.3$, $\gamma = 0.76$) were taken from the literature.[46] For the trehalose-like material, the values of $T_g$ (393 K) and $\gamma$ (0.80) were taken from the same literature source,[46] but this literature value[46] for $D$ did not give power–time curves that agreed with experimental trehalose data.[24] Thus, the value of $D$ used in the simulations (14.8) was chosen to provide power–time curves close to the experimental values.

The simulation values of $\Phi(t)$ were used to construct power–time data, $P(t)$ by numerical differentiation of $\Phi(t)$ and use of the expression,

$$P(t) = \Delta H_\infty \cdot \frac{d\Phi}{dt} \tag{19}$$

$$\Delta H_\infty = H_{\mathrm{ex}}(0, T) = (T_f^0 - T_a) \cdot \Delta C_p$$

where $\Delta H_\infty$ is the relaxation enthalpy for a system relaxing to complete equilibrium. Frequently, the evaluation of $\Delta H_\infty$ is written in terms of the temperature difference $(T_g - T_a)$, as in eq. 5. However, that practice assumes the fictive temperature in the glass is essentially the same as the glass transition temperature, which is often a good approximation but is not exact. Thus, we use eq. 19 in this simulation. Because is found that the power–time curve is normally better represented by the derivative version of the "modified stretched exponential" (MSE) function[24] than by the derivative version of the KWW equation, we fit the derivative version of the MSE function,

$$P = \frac{\Delta H_\infty}{\tau_0} \cdot \left(1 + \frac{\beta t}{\tau_1}\right) \cdot \left(1 + \frac{t}{\tau_1}\right)^{\beta - 2} \phi_{\mathrm{MSE}} \tag{20}$$

to the simulated power–time data to obtain $\beta$, $\tau_0$ and $\tau_1$. The value of $\beta$ corresponds directly to the $\beta$ in the KWW equation while the equivalent of the KWW relaxation time, denoted $\tau_D$, is given by eq. 9. We also fit the KWW equation, eq. 2, to the simulated $\Phi$ data to obtain the parameters, $\tau$ and $\beta$.

The increase in relaxation time during aging is illustrated by Figure 2 for both sucrose-like and trehalose-like materials at 40 and 50°C. Note that the estimated relative increase in relaxation time over 100 h varies with the initial relaxation time from a factor of 1.5 for a trehalose-like material at 40°C (initial $\tau = 3.2 \times 10^5$ h) to a factor of 80 for a sucrose-like material at 50°C (initial $\tau = 29$ h).

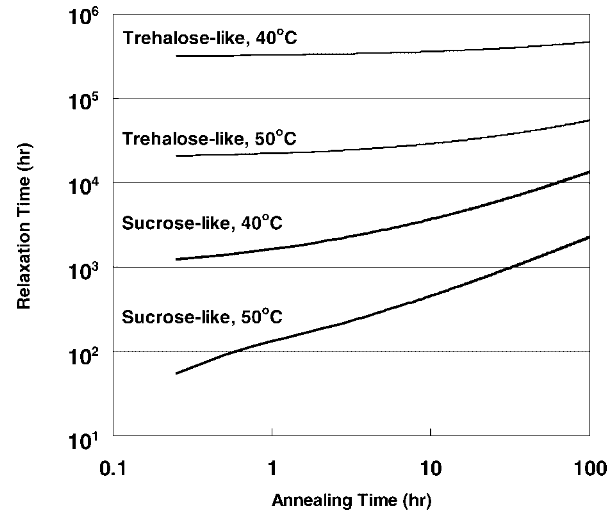


**Figure 2.** Increase in structural relaxation time during annealing disaccharide-like materials at selected temperatures. All simulated data were obtained using an input value of 0.5 for beta. The type of materials and the annealing temperature are indicated in the figure.

Thus, for some materials, the assumption of a constant relaxation time during the enthalpy relaxation experiment is not even a good approximation, particularly when the initial value of relaxation time is on the order of the experiment time or shorter.

For both the MSE fit and the KWW fit, the resulting parameters were compared with the initial values used in the simulation. The relaxation time comparisons are given in Figure 3, where the ratios of the "fit" relaxation time ($\tau$ or $\tau_D$) to the initial relaxation time of the system are provided. It is obvious that the relaxation time determined from the data analysis is much greater than the initial relaxation time, particularly for the sucrose-like systems where the value of $\tau$ or $\tau_D$ from the regression analysis is more than an order of magnitude greater than the initial relaxation time (i.e., the initial value used in the simulation). The effect is generally somewhat greater for analysis of power data than for the corresponding analysis of the $\Phi$ data. The "fit" $\tau$ values may be regarded as approximately the "averaged" values during the annealing period. However, this interpretation is not exact, because the rank orders of the "averaged $\tau$" (according to Fig. 2) and the "fitted $\tau$" are different. Nevertheless, this analysis indicates that the experimentally obtained $\tau$ values will depend greatly on the annealing period employed.

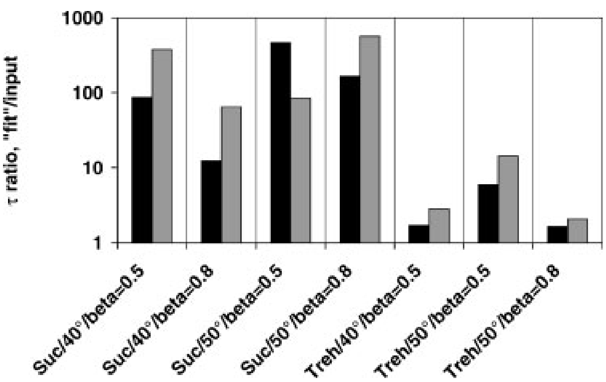


**Figure 3.** Effect of relaxation during the measurement on the measured relaxation time: comparison of the "input" relaxation time of the system with the relaxation time values determined by a fit of the MSE equation (striped bars) or KWW equation (solid bars) to the simulation data. Data are ratios of "fit" relaxation time to "input" relaxation time. The notation, "Suc/40°/beta = 0.5," means data for the sucrose-like system at an annealing temperature of 40°C using an input beta value of 0.5. The annealing period was 100 h.

The comparisons of β are given by Figure 4. Clearly, the values of β obtained from the regression analysis are lower than the input or true initial values (i.e., the β ratios are less than unity), but as one might expect, the error in β decreases as the extent of relaxation during measurement decreases (i.e., as Φ at the end of the annealing run approaches unity). In principle, to the extent the simulation results are accurate, one could use the data given in Figure 4 to correct the β values given by the regression analysis to true values. It should be emphasized that data from the regression analysis gives β values that are too low and τ values that are too high. As shown in Figure 5, the relaxation time constant "on the stretched time scale," $\tau^{\beta}$ obtained from analysis of the data is nearly invariant to the relaxation errors. That is, the values of $\tau^{\beta}$ obtained by fit of either the MSE function to power data or fit of the KWW function to Φ data are nearly the same as the "input" or initial values of $\tau^{\beta}$. Thus, while the usual experimental procedures for evaluation of τ often give very large errors due to relaxation during the measurement, the time constant, $\tau^{\beta}$, is relatively constant. Table 1 shows the impact of the experimental annealing period on the KWW parameters, in which the notation "experimental period" means the maximum annealing time employed in each study. These data clearly show that the experimental design (i.e., the duration of annealing) has a significant effect on the individual KWW parameters, τ and β, but the relaxation time constant, $\tau^{\beta}$, remains largely invariant to annealing times. In all cases, a longer annealing time provided larger τ values and smaller β values. Finally, because $\tau^{\beta}$ is invariant, and because one may obtain an estimate of the reliable β from the data shown in Figure 4, one may also obtain an estimate of the "true" or initial value of τ (or $\tau_D$). Employment of $\tau^{\beta}$ for the comparison of the data is therefore a powerful method by which the effect of the length of the annealing period on τ is reduced. Consequently, attention should focus on $\tau^{\beta}$ to avoid systematic errors in and the misinterpretations that might result from such errors.

**Table 1.** Impact of Experimental Periods on Relaxation Times

| | $t_a$ (h) | τ (h) | β | $\tau^{\beta}$ |
|---|---|---|---|---|
| Indomethacin ($T_g = 43°C$, $T_a = 30°C$) | 2 | 7.63 | 0.55 | 3.04 |
| | 4 | 9.71 | 0.49 | 3.05 |
| | 6 | 9.42 | 0.50 | 3.04 |
| | 16 (ref. 9) | ca. 40 | N/A | N/A |
| Nifedipine ($T_g = 43°C$, $T_a = 30°C$) | 2 | 8.08 | 0.62 | 3.65 |
| | 4 | 9.26 | 0.58 | 3.64 |
| | 6 | 12.70 | 0.48 | 3.38 |
| Maltose ($T_g = 99°C$, $T_a = 83°C$) | 2 | 5.84 | 0.84 | 4.39 |
| | 3 | 6.08 | 0.82 | 4.40 |
| | 5 | 9.48 | 0.65 | 4.28 |
| Maltose ($T_g = 99°C$, $T_a = 91°C$) | 2 | 0.91 | 0.49 | 0.95 |
| | 3 | 0.94 | 0.46 | 0.97 |
| | 5 | 0.97 | 0.43 | 0.99 |

$t_a$: experimental period (i.e., maximum annealing time); onset values were presented as $T_g$.

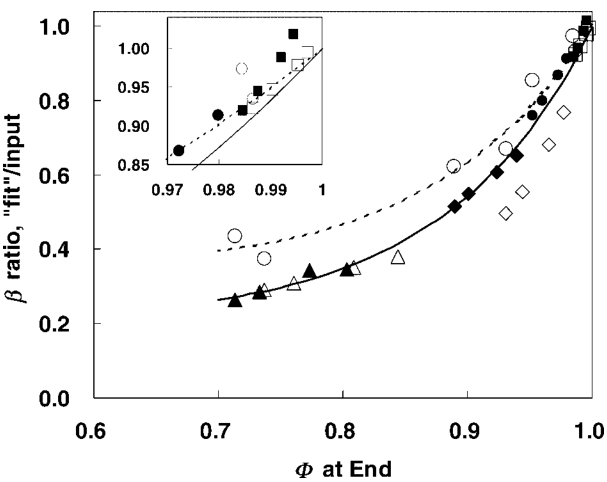


**Figure 4.** Extent of relaxation and value of β from the analysis of simulation power and Φ data according to the MSE equation and KWW equation, respectively. The ratio of the β value from the fit to the value used in the simulation is given as a function of the relaxation function, Φ. Symbols key, MSE fit results: filled diamonds = sucrose-like at 40° with β input = 0.5; open diamonds = sucrose-like at 40° with β input = 0.8; filled triangles = sucrose-like at 50° with β input = 0.5; open triangles = sucrose-like at 50° with β input = 0.8; filled squares = trehalose-like at 40°C with β input = 0.5; filled circles = trehalose-like at 50°C with β input = 0.5; open squares = trehalose-like at 50°C with β input = 0.8. Symbols for data corresponding to the KWW Φ fit are open circles. The dashed line is the "best fit" representation of the KWW Φ fit data, β ratio = 8.08exp(−9.47 Φ + 7.38 $\Phi^2$). The solid line is the "best fit" representation of the MSE power fit data, β ratio = 3.97·exp(−9.7 Φ + 8.32 $\Phi^2$). Here, the sucrose-like data at 40°C with input β = 0.8 seems abnormal and was omitted from the fit. The data for the MSE fit represent data at 99.5, 62.5, 25, and 12.5 h, while only the data at 99.5 h are given for the KWW results. Inset is an expansion of the region near Φ = 1.

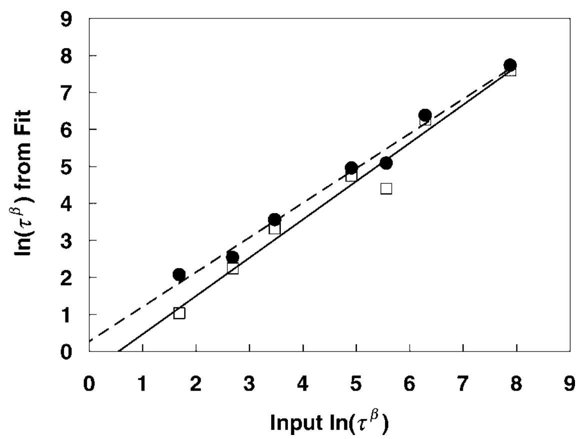


**Figure 5.** Effect of relaxation during the measurement on the measured relaxation time constant on the stretched time scale, $\tau^{\beta}$. Symbols key: circles = values determined from a fit of the KWW equation to the simulation Φ data; squares = values determined from a fit of the derivative of the MSE equation to simulation power data; dashed line = best linear fit to the Φ results; solid line = best linear fit to the power results.

## INVESTIGATION OF THE RELAXATION BY MTDSC

### General

As discussed earlier, DSC can be used to characterize relaxation behavior by measuring the enthalpy recovery during a heating scan that follows selected annealing periods. Recently, modulated-temperature DSC (MTDSC) has been widely used for the characterization of amorphous solids,[13,15,17,18] largely because MTDSC can clearly separate the apparent heat capacity change at the glass transition from the endotherm arising from enthalpy recovery. However, it has been claimed that MTDSC may provide quantitatively different results from those obtained from conventional DSC because the temperature dependence of the "reactivity" or irreversible processes is not properly represented.[47] That is, if the activation energy for the process is large, the mean reactivity over a range of temperatures oscillating around a mean can be different from the reactivity at the mean temperature, because of the nonlinearity. However, this effect is normally very small because in most MTDSC applications, the temperature oscillations are very small in amplitude. In this review, we discuss only practical aspects of the application of MTDSC to relaxation studies. In particular, mathematical detail is held to a minimum. Some phenomena characteristic of the MTDSC experiment, such as the frequency effect and increase of $T_g$ after annealing, which have been largely ignored in the pharmaceutical literature, are discussed here.

### What Effects Contribute to the Apparent Enthalpy Recovery Values?

We must always keep in mind the fact that MTDSC provides a direct measure of enthalpy recovery, not enthalpy relaxation, and factors other than enthalpy relaxation may contribute to the endotherm observed near $T_g$ in the nonreversing signal. The most significant factor, unique to MTDSC, is the "frequency effect."[14,16,19,48–51]

This "frequency effect" is completely unrelated to enthalpy relaxation or recovery, and makes a substantial contribution to the endotherm, thereby leading to the overestimation of enthalpy recovery. As long as the same sample is used (for several experiments) and the experimental conditions are fixed, the frequency effect contribution is nearly constant. However, to maintain constant experimental conditions, care should be taken to use samples of the same size and density.[48,49] The cooling scan is often used to evaluate the frequency effect. However, because cooling scan data are normally less precise than heating data, this procedure tends to introduce significant random error in the final enthalpy recovery data. One may obtain a deeper understanding of the frequency effect from refs. 48 and 49.

Relaxation during the experimental procedure is another factor.[51] In other words, the material can relax even during the temperature scans. This effect may be more important for MTDSC analysis, because MTDSC protocols employ lower scan rates than the conventional DSC experiment. Figure 6 shows a typical thermal program used for relaxation studies. The material is usually first heated above $T_g$ and annealed at that temperature for 3–5 min to erase its thermal history, followed by the quenching and subsequent annealing process at $T_a$ and the heating scan measurement. Figure 7 shows the enthalpy recovery $H_r$ of maltose glass ($T_g = 99°C$, onset value) obtained by this thermal program with different annealing temperatures, when the duration of the annealing step was set to 0 h. It is obvious that apparent enthalpy recovery was observed without any time spent in annealing,

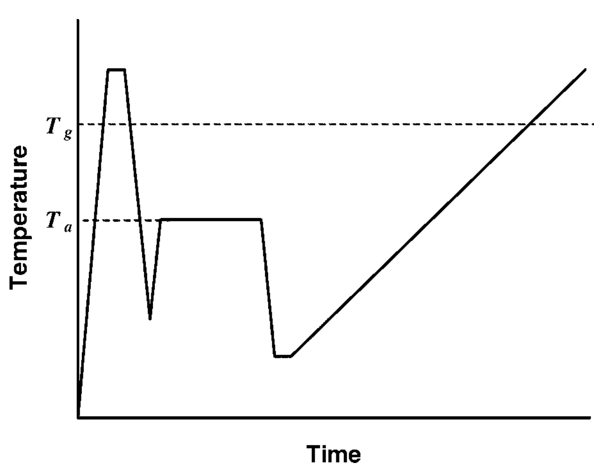


**Figure 6.** Typical DSC protocol for a relaxation study. $T_g$ is the glass transition temperature, and $T_a$ is the annealing temperature.

and the effect increased as the annealing temperature increased. The effect at low temperature is mostly the frequency effect. However, because the frequency effect is relatively insensitive to the annealing temperature, this temperature dependence is not a result of the frequency effect and was likely due to the relaxation during the scan processes (e.g., during the scan to the selected annealing temperature). In other words, residence at high temperature such as 95°C, even though the time period was less than several minutes, seemed to be sufficient to cause some relaxation. In this maltose example, nearly 20% of the excess enthalpy has already been lost during the temperature scan process for a scan to 95°C ($T_g - 4°C$). We note that enthalpy loss during scan steps is typically much less because one normally is not carrying out annealing so close to the glass transition temperature. However, the enthalpy loss during the temperature changes, as well as the frequency effect, must be subtracted from the observed endotherm in the nonreversing signal prior to analyzing the data in terms of the KWW kinetic model. In our opinion, the best method for correcting the raw endotherm area data is to simply subtract the apparent enthalpy recovery value obtained with zero annealing time from the values obtained for nonzero annealing times. That is, do not bother with the separate measurements of frequency effect and temperature scan effects because all that is needed is the sum of the two effects, which is easily and precisely measured as described by Figure 7.

It should also be emphasized that a study of relaxation by DSC analysis is based on the assumption that the relaxation and the recovery enthalpies are identical. However, this assumption is valid only if the enthalpy recovery event is centered at $T_g$ where recovery to the equilibrium state (i.e., line "c," Fig. 1) involves the same energy as enthalpy relaxation (i.e., line "a," Fig. 1). Obviously (Fig. 1), recovery to equilibrium at any temperature other than $T_g$ will involve a different energy.[25] The recovery enthalpy becomes smaller than the relaxation enthalpy if the recovery occurs well below $T_g$ and vice versa. Enthalpy recovery occurs at a temperature where the system requires sufficient mobility to return to the equilibrium state, which is normally at $T_g$. Although the molecular mobility at $T_g$ (i.e., the value of $\tau$) is usually thought of (defined sometimes) as a constant (i.e., $\tau$ is around 100 s for all materials), $\tau$ at $T_g$ does vary with the material,[52] and the mobility required to return to equilibrium will

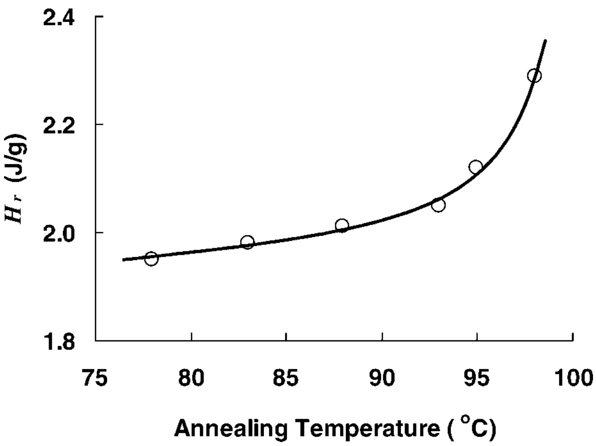


**Figure 7.** Enthalpy recovery values of maltose glass obtained by the thermal program shown in Figure 6 with zero annealing time. The rapid heating and cooling were done at 20°C/min, and the analysis at 2°C/min with ± 0.5°C amplitude, 60-s modulation period. $T_g$ of maltose (onset value) was 99°C under the same analysis conditions. Sample weight was 7 ± 0.5 mg, and it was compressed into disk shape of thickness around 2 mm.

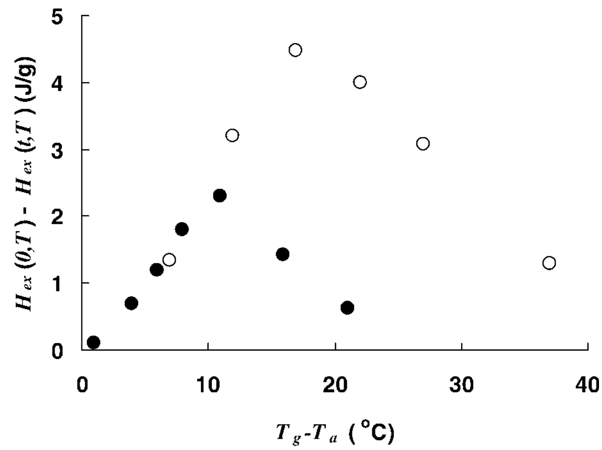


**Figure 8.** The relaxation enthalpy values after 1-h annealing of indomethacin (open, Fukuoka et al.[8]) and maltose (filled).

vary between materials (i.e., the value of τ required will vary). Therefore, plausible explanations do exist for variation between materials in the relationship between $T_g$ and the temperature of the recovery endotherm. The impact on enthalpy recovery of an increase in $T_g$ caused by annealing will be discussed later.

## Estimation of the Initial Excess Enthalpy, Denoted $H_{ex}(0, T)$ or $\Delta H_\infty$

The relaxation rate is governed by the relaxation time, the stretched exponent, and the value of the excess enthalpy of the glass at the start of the annealing experiment. Figure 8 shows the relaxation enthalpy of indomethacin and maltose after 1 h of annealing time at the indicated temperature. One may expect that this value would increase ith a decrease of annealing temperature from eq. 5 or 19. However, maximum values of enthalpy relaxation were observed in a temperature range 10 to 20°C below $T_g$. Closeness to $T_g$ means small relaxation time and therefore rapid relaxation. Thus, one has a maximum. The difference in peak location mainly comes from the difference in the activation energy of the relaxation time. Because the activation energy for structural relaxation in indomethacin is roughly half that for sugars,[9] the difference in the temperature between $T_g$ and the temperature where the maximum relaxation occurs is larger for indomethacin, as shown in Figure 8.

The initial excess enthalpy value is required for calculating the relaxation function, ϕ, from enthalpy recovery data. Although an estimate of the initial excess enthalpy can be obtained by eq. 5, use of this relationship poses some problems. The most apparent problem, which is widely recognized but not well discussed, is the temperature dependence of the heat capacity. The heat capacity is well known to increase with the increase of the temperature both in the glass and supercooled liquid region above $T_g$, although not necessarily with exactly the same temperature dependence.[46] Figure 9 shows the heat capacity of amorphous maltose with its corresponding relative enthalpy values, which were obtained by integrating the raw heat capacity data from the end of the glass transition region. Enthalpy values for the equilibrium glass state (light line) were calculated by simply extrapolating the heat capacity data above $T_g$ to the temperature range below $T_g$, followed by integrating this extrapolated heat capacity data. The difference between the relative enthalpy values for the glass (heavier line) and the equilibrium glass (light line) is the initial excess enthalpy. As indicated earlier, the initial excess enthalpy is generally estimated from eq. 5, where the temperature dependence of heat capacity is assumed identical for both glass and liquid, and so $\Delta C_p$ is taken independent of temperature and is measured at $T_g$. It is obvious from eq. 5 that depending on the definition of $T_g$, different values of initial excess enthalpy will be obtained, and these differences will be relatively greater for

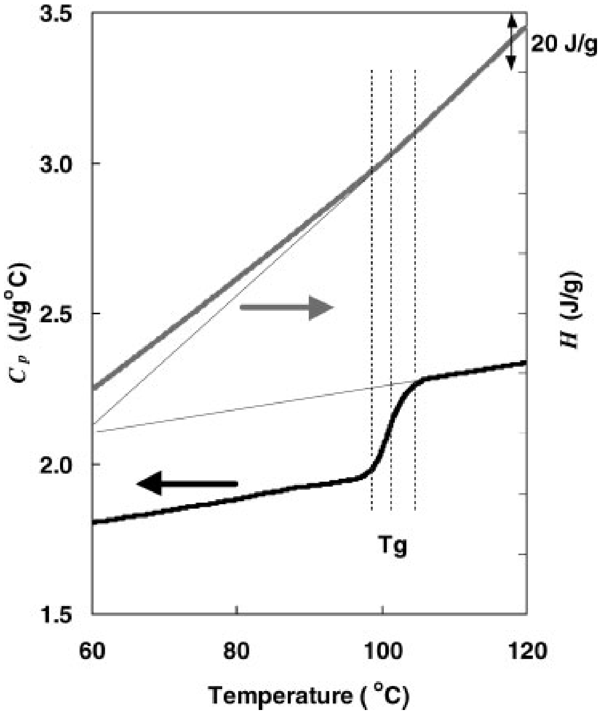


**Figure 9.** The heat capacity of maltose glass obtained by 2°C/min heating scan with the same modulation conditions as for Figure 7 (thick black line), and the calculated enthalpy values by integrating the heat capacity data (thick gray line). The enthalpy of the equilibrium glass (thin gray line) was calculated by simply extrapolating the heat capacity data of the supercooled liquid state to the lower temperature (thin black line). The three candidate temperatures for $T_g$ (onset, midpoint, and end point) are also indicated as dashed lines.

temperatures near the glass transition region. There are three candidates for definition of the glass transition temperature; onset, middle, and end point. Figure 10 shows the initial excess enthalpy values obtained by integrating the raw heat capacity data (i.e., the "correct values," shown by the heavy curved line), compared to values calculated from eq. 5 using three different $T_g$ values. It appears best to choose onset or midpoint $T_g$ for use in eq. 5, but as long as the temperature of interest, $T_a$, is about 30°C or more below the onset of $T_g$, any of the above definitions of $T_g$ could be used without introducing a serious relative error. However, results are very sensitive to the calculation procedure when evaluating initial excess enthalpy near the glass transition region. For example, use of the onset value in eq. 5 for analyzing relaxation at 95°C leads to an underestimation of 0.6 J/g in excess enthalpy compared to the directly integrated value, which corresponds to a

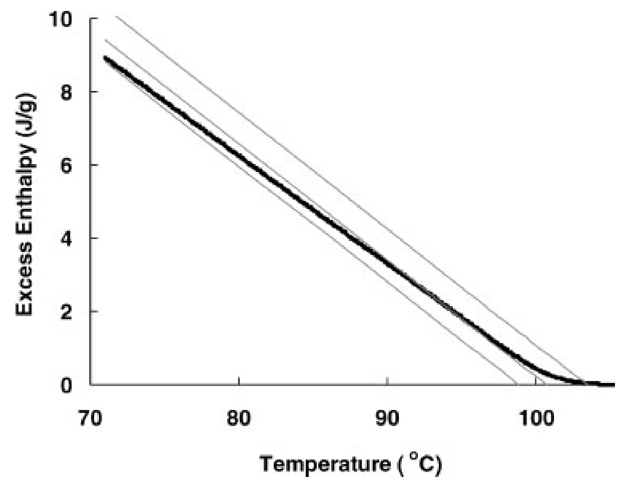


**Figure 10.** The excess enthalpy values of maltose glass obtained by the direct integration of the raw heat capacity data (thick line). The estimation of the excess enthalpy values by eq. 5, using the onset, midpoint, and end point values (bottom to top), are also shown by the thin lines.

relative difference of 33%. Obviously, just below $T_g$, use of the midpoint in eq. 5 is best. Finally, one must recognize that at least with materials that are not prepared by a fast quench from the melt, it is far better to base the calculation of initial excess enthalpy on the initial fictive temperature, as described in eq. 19, provided the initial fictive temperature is known.

## The Relaxation Function $\phi$: Impact of Increase in $T_g$ Caused by Annealing

The relaxation function $\phi$ can be evaluated from

$$\phi(t,T) = \frac{H_{\mathrm{ex}}(t,T)}{H_{\mathrm{ex}}(0,T)} \quad (21)$$

where the excess enthalpy, $H_{\mathrm{ex}}(t, T)$ can be estimated from DSC data by subtracting the enthalpy recovery value from the initial excess enthalpy. However, the usual use of eq. 5 evaluate initial excess enthalpy assumes that annealing does not affect $T_g$. However, the glass transition temperature is slightly increased by annealing.[8,46] Figure 11 shows an example of the impact of annealing on $T_g$. It is obvious that the annealing process raises $T_g$, meaning that the calculated initial excess enthalpy is too small once annealing has progressed. The overestimation of the excess enthalpy due to the $T_g$ shift can be corrected for by

$$H_{\mathrm{ex}}(0,t) - H_{\mathrm{ex}}(t,T) = H_r(t,T) - \Delta C_p \Delta T_g(t,T) \quad (22)$$

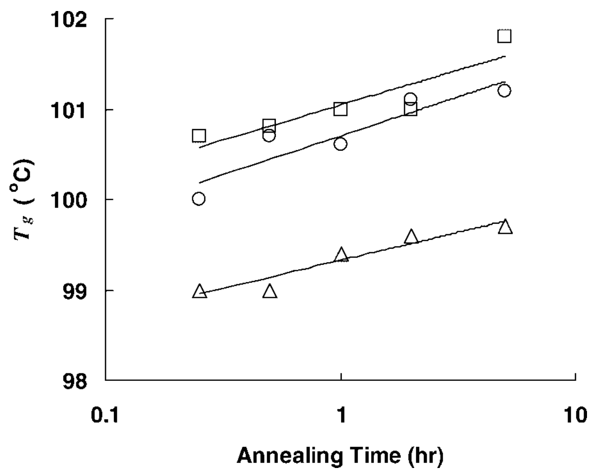


**Figure 11.** The change of the onset $T_g$ of maltose glass after annealing for selected times. The annealing temperatures were 83°C (circle), 88°C (square) and 95°C (triangle).

where $\Delta T_g(t,\ T)$ is the increment of $T_g$ by the annealing. Combining the eqs. 5, 21, and 22, we obtain

$$\phi(t, T) = 1 - \frac{H_r(t, T) - \Delta C_p \Delta T_g(t, T)}{\Delta C_p (T_g - T)} \qquad (23)$$

Figure 12 shows calculated $\phi$ values and their analysis by the KWW equation with or without the $\Delta C_p \Delta T_g$ term correction. The midpoint $T_g$ value was used for the initial excess enthalpy calculation for both methods because it provides the most accurate values at high temperatures. This figure clearly shows that the $\Delta T_g$ correction can significantly impact the results of the analysis when relaxation relatively close to $T_g$ is being studied.

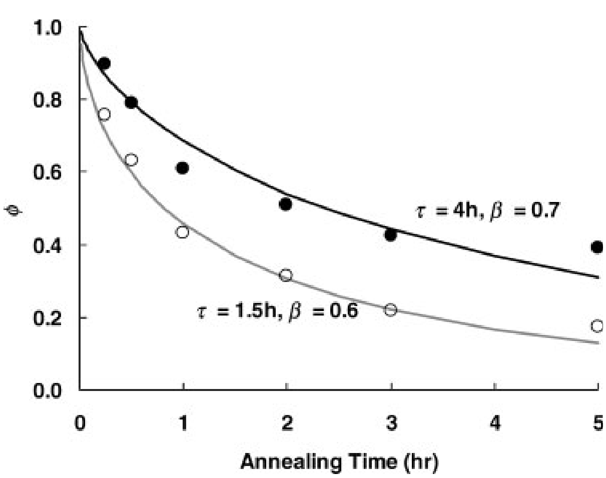


**Figure 12.** The relaxation function $\phi$ as a function of time and their fit by the KWW equation with (filled) or without (open) the $\Delta C_p \Delta T_g$ term correction. The annealing temperature was 88°C, and the midpoint $T_g$ was used for the calculation. The solid lines represent the "best fit" values from the KWW equation. The KWW parameters obtained by the fit are indicated in the figure.

### Relaxation in the Glass Transition Region

Although the relaxation behavior at temperatures just below $T_g$ has less practical importance for pharmaceutical stability research, it is of fundamental interest. However, relaxation studies in this temperature region are beset with difficulty. For example, Figure 13 shows the decay function $\phi$ of a maltose glass in the glass transition region, calculated in the same manner as for Figure 12 and using eq. 23 for $\phi$. Because the onset $T_g$ is around 99°C, these annealing temperatures were only 4 or 6°C below the $T_g$ onset. These $\phi$ values show no obvious time dependence, but yet appear to be significantly less than unity. As the relaxation times in this temperature region are expected to be on the order of 1 h or less, relaxation might have already been completed and the systems might have reached equilibrium. However, if this interpretation is correct, it means that the eq. 5 is significantly in error when used for annealing temperatures close to the glass transition region. Various speculations may well be possible, but the major point is that relaxation studies in the glass transition region are poorly understood at this time, and one should avoid applying the conventional relaxation theory to relaxation studies in the glass transition region.

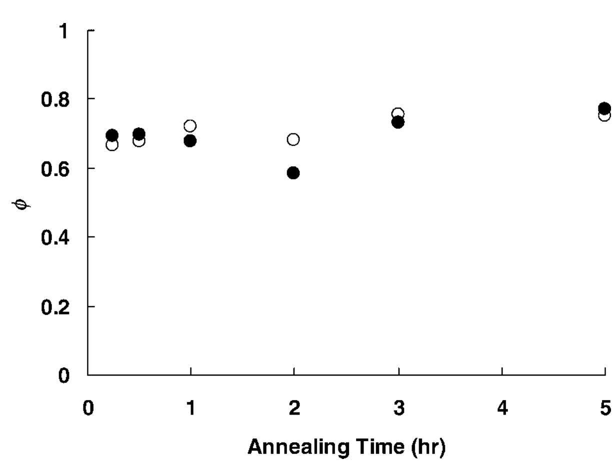


**Figure 13.** The time dependence of the relaxation function $\phi$ of maltose glass at 93°C (filled) and 95°C (open).

### Summary

The application of MTDSC to the analysis of enthalpy relaxation to determine structural relaxation time was discussed. The MTDSC experimental procedure can be very simple, because erasure of previous thermal history can be included together in the analysis program, and the sample can be used repeatedly if sufficiently chemically stable. However, one must keep in mind that the observed quantity is enthalpy recovery and not the relaxation enthalpy, and corrections to the raw data are normally needed, particularly for the "frequency effect." Because small variations in sample form and experimental procedure may impact the magnitude of the frequency effect, care must be exercised in correcting data for this effect. Relaxation during the temperature changes that are a part of the annealing and analysis program also may be significant. The easiest and perhaps best practice is to use the protocol with zero time allocated for annealing to correct for both the frequency effect and relaxation effects during the "nonannealing" parts of the program. Some problems concerning $T_g$, that is, its increase after annealing and its selection for calculating $H_{ex}(0,T)$ were extensively discussed. It is very difficult to provide a foolproof recipe for facing these problems at this point in time, because the glass transition itself is not completely understood. Nevertheless, attention to these matters is required for the proper evaluation of experimental results. Finally, ambiguities and anomalies plague MTDSC studies of relaxation near $T_g$, and such studies should not be analyzed with conventional relaxation theory.

## INVESTIGATION OF THE RELAXATION BY ISOTHERMAL MICROCALORIMETRY

### General

The isothermal microcalorimeter provides a very sensitive and direct measure of the rate of energy loss (or gain) during annealing. Normally, with annealing temperatures well below $T_g$, the sample loses energy in the approach to equilibrium (enthalpy relaxation), but at temperatures closer to $T_g$, equilibrium represents higher energy for many samples, and the approach to equilibrium involves an increase in energy (enthalpy recovery). Enthalpy recovery studies with isothermal microcalorimetry have been introduced relatively recently[25] and the information available in the literature is sparse. The generated heat flow $P$ can be fit by the differentiated form of the KWW equation, eq. 3,

$$P = H_{ex}\left(\frac{\beta}{\tau}\right)\left(\frac{t}{\tau}\right)^{\beta-1}\phi_{KWW} \tag{24}$$

Unlike MTDSC, it is difficult to control the thermal history precisely in microcalorimetry studies because sample preparation must be accomplished outside the instrument and relatively large samples are required. Thus, this instrument is most useful for samples "as is," but because the fictive temperature may vary between samples if the thermal history is not well controlled, obtaining reproducible results requires careful sample handling. As discussed earlier, the KWW equation cannot be applied in the short time range. Because $\beta < 1$, the derivative giving power, eq. 24, approaches infinity as time approaches zero, a clearly unacceptable feature that has an impact on the data analysis, particularly for systems with long relaxation times. In such cases, the fit of eq. 24 to the data is often poor, and therefore as an alternative, the differentiated form of the MSE equation can be used[24] (i.e., eq. 20). Generally, even when the derivative form of the KWW equation does not fit the data well, the derivative form of the MSE equation (eq. 20) does fit the data well and does provide physically reasonable relaxation parameters. In addition, it was found[24] that because experimental errors in $\tau$ and $\beta$ are opposite in sign, the values of $\tau^\beta$ are more "robust," and it was recommended that values of $\tau^\beta$ be reported and compared, rather than values of $\tau$. The simulation results reported earlier in the present work indicate that, in fact, the values of $\tau$ and $\beta$ evaluated by analysis of annealing data are too large and too small, respectively, with the value of $\tau^\beta$ being more reliable. Thus, the simulation results support the empirically based recommendation[24] that $\tau^\beta$ generally should be the value reported and compared. However, the simulations did suggest that knowledge of the extent of relaxation during the study should allow an estimate of the true value of $\beta$, which in turn, would mean that this true value of $\beta$ and the more reliable value of $\tau^\beta$ would allow estimation of a more reliable value of $\tau$. This methodology has yet to be used in practice.

There is little detailed knowledge regarding the recovery process itself, although the process is suggested to be "autocatalytic."[53,54] As noted above, this process can also be observed by microcalorimetry. If the amorphous material has relaxed to some extent, its fictive temperature, $T_f$, should be well below $T_g$. If the material is allowed to age above its $T_f$, it recovers toward the equilibrium glassy state, which is higher in energy, thereby producing an endothermic heat flow. We will return to this subject later with some experimental observations.

## Enthalpy Relaxation Data

Figure 14 shows enthalpy relaxation kinetics of sucrose glass observed with the isothermal microcalorimetry and the fit by the differentiated form of either the KWW equation (50°C data) or the MSE equation (30°C data), where eq. 5 was used to calculate the excess enthalpy values. The 30°C data is better fit by the derivative form of the MSE equation than by the corresponding KWW equation. For both data sets, the fit is quite good.

The $\tau$ values obtained by both DSC enthalpy recovery measurements and isothermal microcalorimetry are compared in Figure 15. A comparison of $\tau^{\beta}$ would have been desirable, but the key literature data[9] does not give individual $\beta$ values. In general, the $\tau$ values obtained by isothermal microcalorimetry are in satisfactory agreement with the corresponding data obtained by DSC,

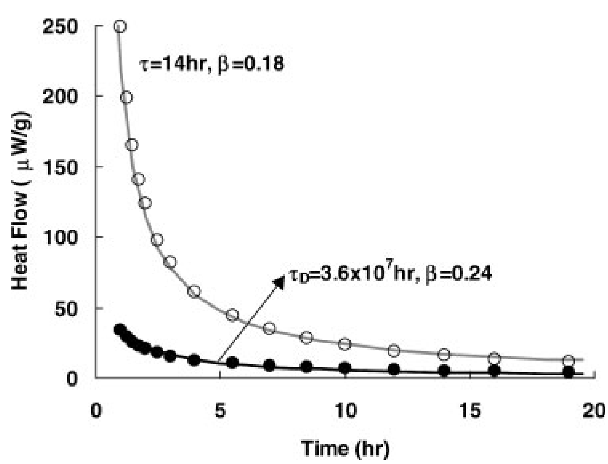


**Figure 14.** Isothermal microcalorimetry heat flow during enthalpy relaxation of sucrose glass at 50°C (open) and 30°C (filled) and the fits to the derivative form of the KWW equation (50°C) or the derivative form of the MSE equation (30°C). $T_g$ of the sucrose glass is around 77°C.[9] These sucrose glasses were prepared by freeze drying, followed by the erasure of the thermal history by the annealing at 80°C (above the $T_g$) for 30 min. The solid lines represent the "best fits" from the derivative forms of the KWW or MSE equations. The relaxation times and beta values resulting from the data analysis are given on the figure.

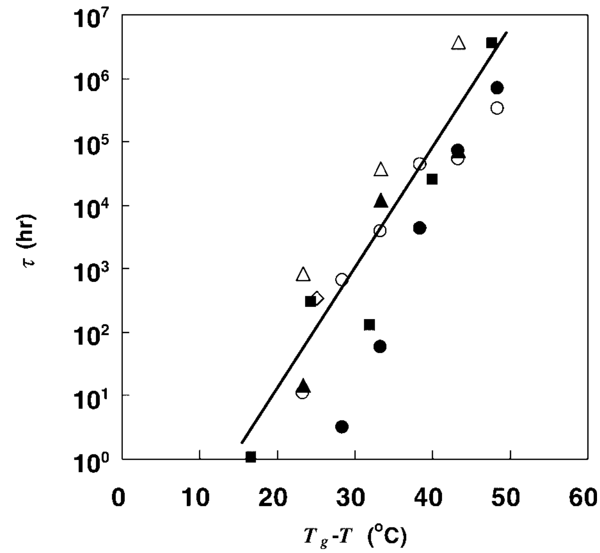


**Figure 15.** Comparison of the relaxation times for sucrose glasses quenched from the melt. Symbols key: data as obtained by DSC (filled squares, Hancock et al.[9]; open diamond, Liu et al.[24]) or isothermal microcalorimetry (Liu et al.[24], Pikal et al.[43]) where the open triangles represent $\tau_D$ from the MSE equation and the filled triangles represent $\tau$ from the KWW equation. The relaxation times for sucrose glass prepared by freeze drying[55] are also shown. The open circles represent $\tau_D$ from the MSE equation and the filled circles represent $\tau$ from the KWW equation. The thick straight line is drawn through the DSC data as a representation of the average DSC enthalpy recovery data for $\tau$. The values of $\beta$ from the KWW analysis of DSC data were stated to be 0.4–0.8[9] and 0.3.[24] The values of $\beta$ obtained from the isothermal calorimetry data[24,43,55] were about 0.2.

particularly when one considers the possible bias caused by variable length of the annealing period causing variation in $\tau$ and $\beta$ values. For isothermal calorimetry data, values of $\tau_D$ from the MSE equation seem to have less scatter and are usually larger than corresponding $\tau$ values from the KWW equation. It should be noted that the relaxation times for the samples prepared by freeze drying have significantly smaller relaxation times than samples prepared by quenching from the melt, an observation also noted earlier.[24]

Although a detailed comparison of $\beta$ values is not possible, $\beta$ values from microcalorimetry method were systematically smaller than results from DSC. Whether or not this lack of agreement represents a failing of the equations to represent the data, such as a possible contribution of $\beta$-relaxation to the microcalorimetric power response, is unknown. However, it is clear from the simulation studies provided earlier that at least part of the reason has nothing to do with extraneous relaxation effects such as β-relaxation. The β values obtained from an analysis of simulated enthalpy recovery data (DSC) were also larger than the corresponding values obtained by analysis of the simulation power data (isothermal calorimetry). Thus, at least part of the effect is attributed to the different impact of a time-dependent relaxation time on the measurement for enthalpy recovery than in the relaxation rate measurement by isothermal calorimetry. Additional comparative studies are needed to clarify these issues.

### Investigations above $T_f$ (Enthalpy Recovery Process)

As indicated earlier, isothermal calorimetry can also be used to study enthalpy recovery when the sample is studied at a temperature above its fictive temperature. Figure 16 shows the heat flow from maltose-based amorphous samples observed at various temperatures. In each case, the fictive temperature was 32°C. Note that the samples produced a strong endothermic heat flow at the start of the experiment, presumably arising from the enthalpy recovery process, but later the signal becomes exothermic, at least for the higher temperatures. This endothermic heat flow can be reproduced even when the sample was introduced into the calorimeter from a temperature higher than the calorimeter temperature, thus proving that this endotherm was not due to incomplete thermal equilibration.

The exothermic signal is not easily explained with conventional relaxation theory. One might

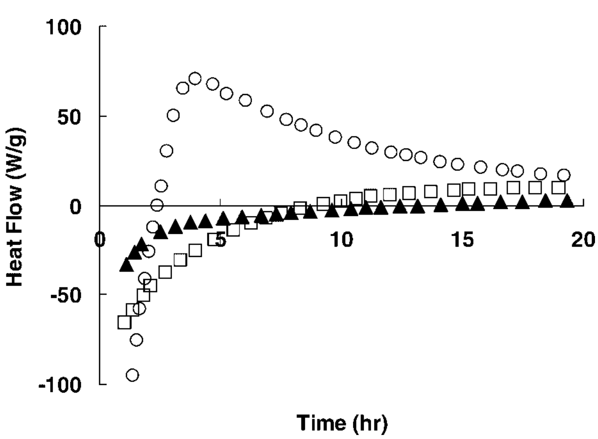


**Figure 16.** The enthalpy recovery of a maltose-based formulation observed by isothermal microcalorimetry at 35 (triangles), 40 (squares), and 45 (circles) °C.[25] $T_f$ of the formulation was 32°C.

speculate that the effect has its origin in the heterogeneity of a system (i.e., distribution of independent substates) that is annealed at a lower temperature and then brought to a higher storage temperature for calorimetric study. With a distribution of states there would also be a distribution of fictive temperatures, which would mean that some substates could have fictive temperatures less than the storage temperature, and some states could have fictive temperatures greater than the storage temperature. The collection of states with the lower fictive temperatures would then increase in energy in moving toward equilibrium, producing endothermic heat flow, and the states with higher fictive temperature would lose energy during aging and produce an exothermic heat flow. Thus, one could have both exothermic and endothermic heat flow from a single sample during aging if the relaxation times are sufficiently different. However, the lower fictive temperature states would have a longer relaxation time than the states with higher fictive temperature (i.e., see eq. 12), and therefore, the heterogeneous state hypothesis would result in an exothermic heat flow (i.e., shorter τ) followed by an endothermic heat flow (i.e., longer τ), which is *not* what is observed experimentally (Fig. 15). Thus, the events must be more complex. One might speculate that perhaps the endothermic process appears first because the τ for the recovery process is much smaller than that for the relaxation process.[25] Alternatively, perhaps these observations reflect differences in thermal history not measured by the fictive temperature, $T_f$. Indeed, there are many observations, classified as the "memory effect"[4,53] that are not adequately explained by conventional relaxation theory. Clearly, the phenomenon is anomalous, and it is our hope that future microcalorimetry studies will help in the understanding of such phenomena.

### Summary

The use of isothermal microcalorimetry for observing both the enthalpy relaxation and recovery processes was discussed. The greatest advantage of this method is that it can provide direct heat flow rates during both relaxation and recovery with very high sensitivity. Even samples having very large relaxation times can be studied with a few days of experimental run time. The relaxation process can be analyzed using the differentiated form of the KWW, but generally the MSE equation should be used in place of the KWW equation, particularly if the relaxation time is very large. Recall that the simulation studies discussed earlier indicate that for both DSC and microcalorimeter data, increases in relaxation time during the annealing cause the $\tau$ and $\beta$ values obtained from the kinetic analysis to be too large and too small, respectively. However, the value of the stretched time constant $\tau^{\beta}$, is not affected by the degree of the relaxation. Isothermal microcalorimetry is better suited to study samples "as is" because thermal history cannot be adjusted by scanning above the $T_g$ as is commonly done with a DSC. The relatively large sample size requirement (usually 50–200 mg) and the limited temperature range (10–80°C) also restrict the types of experiments. Much care should also be taken to avoid changes in moisture content; usually sorption of moisture from the atmosphere by dry samples is the more serious problem. Because moisture sorption and desorption appear as exothermic and endothermic heat flows, respectively,[23] the determination of relaxation time is impacted. Nevertheless, increased use of the microcalorimetry technique should provide a much deeper understanding of enthalpy relaxation and recovery dynamics in glassy systems.

## CONCLUSIONS

The calorimetric methods have been the most convenient ways to investigate structural relaxation in glassy pharmaceutical systems. The use of the two representative methods, MTDSC and the isothermal microcalorimetry, has been discussed in this review by comparing the advantages, problems, and limitations. The MTDSC experiment is very simple, and it requires only very small amounts of sample. However, much care is needed in the quantitative analysis because the observed endotherm is not a direct observation of the relaxation enthalpy. Notably, data must be corrected for the "frequency effect." In addition, the investigation of relaxation behavior near $T_g$ is a difficult issue for MTDSC. Isothermal calorimetry has a great advantage in that this technique directly measures the rate of energy change during relaxation (or recovery, if the fictive temperature is lower than the sample temperature) with very high sensitivity, thereby allowing very slow processes to be studied effectively. In general, the MSE equation should be employed to analyze the data. Disadvantages of isothermal microcalorimetry are the need for a relatively large sample and the limited temperature range of the instrument.

Simulation studies show that because of significant changes in relaxation time during the aging experiment, the values of $\tau$ and $\beta$ obtained by either KWW or MSE analysis are different from the initial values for the sample. The relaxation time, $\tau$, is too large and the stretched exponent, $\beta$, is too small. However, the value of the stretched time constant, $\tau^{\beta}$, is representative of the initial value. We note also, that the value of $\tau^{\beta}$ is also more "robust" (i.e., less sensitive to experimental errors) than $\tau$. Thus, values of $\tau^{\beta}$ should be reported and compared. However, the same simulations also suggest that knowledge of the extent of relaxation during the measurement (i.e., measured by $\Phi$) can be used to correct for the error in $\beta$, and therefore one may perhaps obtain a useful estimate of $\tau$ from the reliable value of $\beta$ and the less variable value of $\tau^{\beta}$.

## REFERENCES


1. Pikal MJ, Lukes AL, Lang JE, Gaines K. 1978. Quantitative crystallinity determinations for β-lactam antibiotics by solution calorimetry: Correlations with stability. J Pharm Sci 67:767–773.
2. Oguchi T, Yonemochi E, Yamamoto K, Nakai Y. 1989. Freeze-drying of drug-additive binary systems. II. Relationship between decarboxylation behavior and molecular states of *p*-aminosalicylic acid. Chem Pharm Bull 37:3088–3091.
3. Guo Y, Byrn SR, Zografi G. 2000. Physical characteristics and chemical degradation of amorphous quinapril hydrochloride. J Pharm Sci 89:128–143.
4. Hodge IM. 1994. Enthalpy relaxation and recovery in amorphous materials. J Non-Cryst Solids 169: 211–266.
5. Ediger MD, Angell CA, Nagel SR. 1996. Supercooled liquids and glasses. J Phys Chem 100: 13200–13212.
6. Angell CA, Ngai KL, McKenna GB, McMillan PF, Martin SW. 2000. Relaxation in glassforming liquids and amorphous solids. Appl Phys Rev 88: 3113–3157.
7. Sasabe H, Moynihan CT. 1978. Structural relaxation in poly(vinyl acetate). J Polym Sci Polym Phys Ed 16:1447–1457.
8. Fukuoka E, Makita M, Yamamura S. 1986. Some physicochemical properties of glassy indomethacin. Chem Pharm Bull 34:4314–4321.
9. Hancock BC, Shamblin SL, Zografi G. 1995. Molecular mobility of amorphous pharmaceutical solids below their glass transition temperatures. Pharm Res 12:799–806.

10. Andronis V, Zografi G. 1998. The molecular mobility of supercooled amorphous indomethacin as a function of temperature and relative humidity. Pharm Res 15:835–842.
11. Koide M, Sato R, Momatsu T, Matusita K. 1995. Viscosity of lead silicate glasses below glass transition tmperature by the fibre bending method. Phys Chem Glasses 36:172–175.
12. Andronis V, Zografi G. 1997. Molecular mobility of supercooled amorphous indomethacin, determined by dynamic mechanical analysis. Pharm Res 14: 410–414.
13. Hill VL, Craig DQM, Feely LC. 1998. Characterization of spray-dried lactose using modulated differential scanning calorimetry. Int J Pharm 161:95–107.
14. Royall PG, Craig DQM, Doherty C. 1998. Characterisation of the glass transition of an amorphous drug using modulated DSC. Pharm Res 15:1117–1121.
15. Verdonck E, Schaap K, Thomas LC. 1999. A discussion of the principles and applications of modulated temperature DSC (MTDSC). Int J Pharm 192:3–20.
16. Craig DQM, Barsnes M, Royall PG, Kett VL. 2000. An evaluation of the use of modulated temperature DSC as a means of assessing the relaxation behavior of amorphous lactose. Pharm Res 17:696–700.
17. Hutchinson JM, Montserrat S. 2001. The application of temperature-modulated DSC to the glass transition region II. Effect of a distribution of relaxation times. Thermochim Acta 377:63–84.
18. Simon SL. 2001. Temperature-modulated differential scanning calorimetry: Theory and application. Thermochim Acta 374:55–71.
19. Van den Mooter G, Craig DQM, Royall PG. 2001. Characterization of amorphous ketoconazole using modulated temperature differential scanning calorimetry. J Pharm Sci 90:996–1003.
20. Sheridan PL, Buckton G, Storey DE. 1995. Development of a flow microcalorimetry method for the assessment of surface properties of powders. Pharm Res 12:1025–1030.
21. Willson RJ, Beezer AE, Mitchell JC, Loh W. 1995. Determination of thermodynamic and kinetic parameters from isothermal heat conduction microcalorimetry: Applications to long-term reaction studies. J Phys Chem 99:7108–7113.
22. Phipps MA, Mackin LA. 2000. Application of isothermal microcalorimetry in solid state drug development. Pharm Sci Technol Today 3:9–17.
23. Kawakami K, Numa T, Ida Y. 2002. Assessment of amorphous content by microcalorimetry. J Pharm Sci 91:417–423.
24. Liu J, Rigsbee DR, Stotz C, Pikal MJ. 2002. Dynamics of pharmaceutical amorphous solids: The study of enthalpy relaxation by isothermal microcalorimetry. J Pharm Sci 91:1853–1862.
25. Kawakami K, Ida Y. 2003. Direct observation of the enthalpy relaxation and the recovery processes of maltose-based amorphous formulation by isothermal microcalorimetry. Pharm Res 20:1430–1436.
26. Götze W, Sjögren L. 1992. Relaxation processes in supercooled liquids. Rep Prog Phys 55:241–376.
27. Rault J. 2000. Origin of the Vogel-Fulcher-Tammann law in glass forming materials: The $\alpha$-$\beta$ bifurcation. J Non-Cryst Solids 271:177–217.
28. Angell CA. 1991. Relaxation in liquids, polymers and plastic crystals—Strong/fragile patterns and problems. J Non-Cryst Solids 131–133:13–31.
29. Phillips JC. 1994. Microscopic theory of the Kohlrausch relaxation constant $\beta_K$. J Non-Cryst Solids 172–174:98–103.
30. Shamblin SL, Hancock BC, Dupuis Y, Pikal MJ. 2000. Interpretation of relaxation time constants for amorphous pharmaceutical systems. J Pharm Sci 89:417–427.
31. Hill RM, Jonscher AK. 1983. The dielectric behavior of condensed matter and its many-body interpretation. Contemp Phys 24:75–110.
32. Privalko VP. 1999. Glass transition in polymers: Dependence of the Kohlrausch stretching exponent on the kinetic free volume fraction. J Non-Cryst Solids 255:259–263.
33. Ngai KL. 1998. Correlation between the secondary b-relaxation time at $T_g$ and the Kohlrausch exponent of the primary $\alpha$-relaxation. Physica A 261:36–50.
34. Ediger MD. 1998. Can density or entropy fluctuations explain enhanced translational diffusion in glass-forming liquids? J Non-Cryst Solids 235–237:10–18.
35. Moynihan CT. 1998. Contributions of dynamic heterogeneity to non-exponential electrical relaxation in ionically conducting glasses and melts. J Non-Cryst Solids 235–237:781–788.
36. Sillescu H. 1999. Heterogeneity at the glass transition: A review. J Non-Cryst Solids 243:81–108.
37. Wang CY, Ediger MD. 2000. Anomalous translational diffusion: A new constraint for models of molecular motion near the glass transition temperature. J Phys Chem B 104:1724–1728.
38. Kovacs AJ, Aklonis JJ, Hutchinson JM, Ramos AR. 1979. Isobaric volume and relaxation recovery of glasses. II. A transparent multiparameter theory. J Polym Sci Polym Phys Ed 17:1097–1162.
39. Hodge IM. 1982. Effects of annealing and prior history on enthalpy relaxation in glassy polymers. 2. Mathematical modeling. Macromolecules 15: 762–770.
40. Montserrat S. 1994. Physical aging studies in epoxy resins. I. Kinetics of the enthalpy relaxation process in a fully cured epoxy resin. J Polym Sci Part B Polym Phys 32:509–522.
41. Peyron M, Pierens GK, Lucas AJ, Hall LD, Stewart RC. 1996. The modified stretched-exponential model

for characterization of NMR relaxation in porous media. J Mag Res Ser A 118:214–220.
42. Hancock BC, Zografi G. 1997. Characteristics and significance of the amorphous state in pharmaceutical systems. Pharm Res 86:1–12.
43. Pikal MJ, Chang L, Tang X. 2004. Evaluation of glassy state dynamics from the width of the glass transition: Results from theoretical simulation of differential scanning calorimetry and comparisons with experiment. J Pharm Sci 93:981–994.
44. Angell CA. 1995. Formation of glasses from liquids and biopolymers. Science 267:1924–1935.
45. Simon SL, McKenna GB. 1997. The effects of structural recovery and thermal lag in temperature-modulated DSC measurements. Thermochim Acta 307:1–10.
46. Shamblin SL, Tang X, Chang L, Hancock B, Pikal MJ. 1999. Characterization of the time scales of molecular motion in pharmaceutically important glasses. J Phys Chem B 103:4113–4121.
47. Johari GP, Ferrari C, Tombari E, Salvetti G. 1999. Temperature modulation effects on a material's properties: Thermodynamics and dielectric relaxation during polymerization. J Chem Phys 110: 11592–11598.
48. Weyer S, Hensel A, Schick C. 1997. Phase angle correction for TMDSC in the glass-transition region. Thermochim Acta 304(305):267–275.
49. Jiang Z, Imrie CT, Hutchinson JM. 1998. Temperature modulated differential scanning calorimetry. Part I: Effects of heat transfer on the phase angle in dynamic ADSC in the glass transition region. Thermochim Acta 315:1–9.
50. Bustin O, Descamps M. 1999. Slow structural relaxations of glass-forming maltitol by modulated DSC calorimetry. J Chem Phys 110:10982–10992.
51. Six K, Verreck G, Peeters J, Augustijns P, Kinget R, Van den Mooter G. 2001. Characterization of glassy itraconazole: A comparative study of its molecular mobility below Tg with that of structural analogues using MTDSC. Int J Pharm 213:163–173.
52. Moynihan CT, Macedo PB, Montrose CJ, Gupta PK, DeBolt MA, Dill JF, Dom BE, Drake PW, Easteal AJ, Elterman PB, Moeller RP, Sasabe H, Wilder JA. 1976. Structural relaxation in vitreous materials. Ann NY Acad Sci 279:15–35.
53. Kovacs AJ. 1963. Transition vitreuse dans les polymères amorphes. Etude phénoménologique. Fortschur Hochpolym-Forsch Bd 3:394–507 (in French).
54. McKenna GB. 1995. Dynamics and mechanics below the glass transition: The non-equilibrium state. Comp Mater Sci 4:349–360.
55. Kawakami K. 2004. Investigation of the structural relaxation process of amorphous formulation by isothermal microcalorimetry. Netsu Sokutei 31: 74–79 (in Japanese).